STEM CELLS®

TISSUE-SPECIFIC STEM CELLS

Regenerative Effects of Transplanted Mesenchymal Stem Cells in Fracture Healing

FROILÁN GRANERO-MOLTÓ,[a] JARED A. WEIS,[a] MICHAEL I. MIGA,[b] BENJAMIN LANDIS,[c] TIMOTHY J. MYERS,[a] LYNDA O'REAR,[c] LARA LONGOBARDI,[a] E. DUCO JANSEN,[b] DOUGLAS P. MORTLOCK,[d] ANNA SPAGNOLI[a,e]

Departments of [a]Pediatrics and [e]Biomedical Engineering, University of North Carolina at Chapel Hill, Chapel Hill, North Carolina, USA; Departments of [b]Biomedical Engineering, [c]Pediatrics, and [d]Molecular Physiology and Biophysics, Vanderbilt University, Nashville, Tennessee, USA

Key Words. Mesenchymal stem cells • Fracture healing • CXCR4 • Bone morphogenic protein 2 • Stem cell niche

ABSTRACT

Mesenchymal stem cells (MSC) have a therapeutic potential in patients with fractures to reduce the time of healing and treat nonunions. The use of MSC to treat fractures is attractive for several reasons. First, MSCs would be implementing conventional reparative process that seems to be defective or protracted. Secondly, the effects of MSCs treatment would be needed only for relatively brief duration of reparation. However, an integrated approach to define the multiple regenerative contributions of MSC to the fracture repair process is necessary before clinical trials are initiated. In this study, using a stabilized tibia fracture mouse model, we determined the dynamic migration of transplanted MSC to the fracture site, their contributions to the repair process initiation, and their role in modulating the injury-related inflammatory responses. Using MSC expressing luciferase, we determined by bioluminescence imaging that the MSC migration at the fracture site is time- and dose-dependent and, it is exclusively CXCR4-dependent. MSC improved the fracture healing affecting the callus biomechanical properties and such improvement correlated with an increase in cartilage and bone content, and changes in callus morphology as determined by micro-computed tomography and histological studies. Transplanting CMV-Cre-R26R-Lac Z-MSC, we found that MSCs engrafted within the callus endosteal niche. Using MSCs from *BMP-2-Lac Z* mice genetically modified using a bacterial artificial chromosome system to be *β*-gal reporters for bone morphogenic protein 2 (BMP-2) expression, we found that MSCs contributed to the callus initiation by expressing BMP-2. The knowledge of the multiple MSC regenerative abilities in fracture healing will allow design of novel MSC-based therapies to treat fractures. STEM CELLS *2009;27:1887–1898*

Disclosure of potential conflicts of interest is found at the end of this article.

INTRODUCTION

High-energy tibia fractures are threatening injuries with slow healing times averaging 43-49 weeks [1]. Furthermore, the fracture healing process is impaired in 10%–20% of fractures, resulting in nonunions and causing severe disabilities [2–4]. Nonunions are treated mostly with bone autografts that are associated with morbidities related to the harvesting procedure, and have a limited supply and unpredictable reparative potential [5]. There is a compelling need to develop novel therapies to improve the fracture healing course and to treat nonunions. Mesenchymal stem cells (MSC) initiate the fracture repair process leading to the formation of a cartilaginous template (callus) that is then replaced by new bone that repairs the gap [6]. Limitation in MSC number and/or functions is hypothesized to play a critical role in the pathogenesis of nonunions. MSC are present in several adult tissues including bone marrow (BM) and are capable of differentiating in vitro into mesenchyme cell types including chondrocytes and osteocytes, although such differentiation has not been unequivocally shown in vivo [7]. Furthermore, both BM-MSC and BM mononuclear cells have been reported to exert beneficial effects in the healing of a limited number of patients with nonunions [8–13]. Although promising, these clinical studies are anecdotal. Before controlled clinical trials can begin, critical animal studies are necessary to determine how MSC are recruited and survive at the fracture site, their repair effectiveness, and the mechanisms through which they exert their actions.

Although MSC seem to migrate into damaged tissues, their dynamic trafficking and tissue homing when systemically infused is a poorly understood process [14–16]. Postmortem microscopy is the standard method to detect transplanted MSC within the tissues; however, it does not allow

Author contributions: F.G.-M.: conception and design, collection and/or assembly of data, data analysis and interpretation, manuscript writing, final approval of manuscript; J.A.W.: conception and design; collection of data, data analysis and interpretation, final approval of manuscript; M.I.M.: data analysis, provision of study material, final approval of manuscript; B.L.: collection of data, data analysis, final approval of manuscript; T.J.M., L.O., and L.L.: collection of data, final approval of manuscript; E.D.J. and D.P.M.: provision of study material, final approval of manuscript; A.S.: conception and design, financial support, collection and/or assembly of data, data analysis and interpretation, manuscript writing, final approval of manuscript.

Correspondence: Anna Spagnoli, M.D., Departments of Pediatrics, Division of Pediatric Endocrinology, 3341 Mason Farm Road, Campus Box: 7039, University of North Carolina at Chapel Hill, Chapel Hill, North Carolina, 27599-7039, USA. Telephone: 919-843-6904; Fax: 919-843-6905; e-mail: spagnoa@med.unc.edu Received January 27, 2009; accepted for publication April 12, 2009; first published online in STEM CELLS *EXPRESS* April 23, 2009. 1066-5099/2009/$30.00/0 doi: 10.1002/stem.103

either to study the cell trafficking or to perform longitudinal observations and it is not quantitative. Small-animal in vivo imaging bioluminescence (BLI) allows to determination of a semiquantitative temporal and spatial analysis and biodistribution of the light signal of luciferase-tagged cells within a living animal. Among chemokines and their receptors, CXCR4 has been found to be critical in hematopoietic stem cell homing and cancer cell metastasis [17]. The CXCR4 expression and contribution to MSC migration in vitro and its need in MSC homing in vivo have been scarcely evaluated [18, 19].

Several reports have shown that MSC delivered to an injured tissue can improve the recovery; however, a limited number of MSC have been demonstrated to differentiate into the repaired tissue [20–22]. This discrepancy might be explained by the fact that (a) there are technical difficulties in identifying MSC within the repaired tissue; (b) studies have focused on the identification of MSC differentiation into cells involved in advanced stages of healing; (c) MSC mechanisms of action, other than differentiation, may have induced the regeneration. Anti-inflammatory paracrine effects of MSC have been reported in animal models of acute and chronic inflammatory diseases [23–26]. Most recently, MSC transplantation in 55 patients with severe graft-versus-host disease has led to a complete response or improvement in 39 patients [27]. It is plausible that due to their intrinsic multipotentiality, MSC have several distinct reparative actions. Uncontrolled inflammation plays a critical role in the pathogenesis of nonunions and a selective modulation of the inflammatory response may become the target of new therapies to enhance bone repair and to prevent the occurrence of a nonunion. The role of MSC in the initiation of the callus formation has been scarcely investigated, and most of the studies have focused on more advanced repair stages either during the cartilaginous callus maturation or the mineralization process [28, 29].

Our studies were designed to determine (a) the in vivo trafficking and homing within the fractured tibia of systemically transplanted MSC; (b) the need of CXCR4 for MSC homing; (c) the effects of MSC transplant in the callus biomechanical properties; (d) the MSC engraftment into the repairing tissue and contribution to the callus initiation; (e) the systemic and local anti-inflammatory effects of MSC in fracture repair.

Materials and Methods

Reagents

7-Amino-actinomycin D was from Molecular Probes Inc. (Eugene, OR, http://probes.invitrogen.com); D-Luciferin, from Biosynth-International (Staad, Switzerland, http://www.biosynth.com).

Antibodies

Biotin-conjugated anti-mouse CD34, CD45, CD11b, and CXCR4 antibodies were from BD Biosciences (San Diego, http://www.bdbiosciences.com). Phycoerythrin-conjugated anti-mouse CXCR4, CD29, CD44, CD73, CD105, and CD45 and control isotype antibodies were from eBioscience (San Diego, http://www.ebioscience.com).

Stabilized fracture model

All animal procedures were approved by the animal care committee of the University of North Carolina-Chapel Hill and Vanderbilt University. Stabilized tibia fractures were produced in 8- to 12-week-old FVB female syngenic mice (FVB-NJ; Jackson Laboratory, Bar Harbor, ME, http://www.jax.org) by intramedullary fixation using a 0.25-mm stainless steel pin (Fine Science Tools, Foster City, CA, http://www.finescience.com) inserted through the patellar tendon inside the medullar canal of the tibia followed by closed fracture using a three-point bending device with a standardized force [30]. For pain control, bupremorphine (0.5 mg/kg) was administered subcutaneously.

Isolation and expansion of MSCs

Primary cultures of BM-MSCs were obtained by flushing the BM from femurs and tibias of 4- to 6-week-old FVB-NJ mice as previously reported [31]. Briefly, BM nucleated plastic-adhering cells were expanded for 7-10 days without passaging [31]. Immediately before transplantation, contaminating hematopoietic cells were eliminated by immunodepletion of the CD45-, CD11b-, and CD34-positive cells using a magnetic-activated cell sorting system (Miltenyi Biotec, Bergisch Gladbach, Germany, http://www.miltenyibiotec.com). As shown in supporting information Figure 1, using this protocol we obtain a MSC population in which $> 90\%$ of cells express the specific MSC markers CD73, CD29, and CD44; and 67.5%, the CD105 marker. Furthermore, MSCs after immunodepletion were negative for CD45 ($0.9 \pm 0.5\%$, $n = 3$) and CD11b ($1.1 \pm 1.3\%$, $n = 3$). For BLI imaging, MSCs were isolated from FVB/N animals constitutively expressing *Firefly luciferase* under the β-actin promoter (FVB/N-Tg(β-*Actin-luc*)-Xen) (Caliper Life Sciences, Hopkinton, MA, http://www.caliperls.com). After fracture, mice received a transplant of 10^6 MSCs by tail vein injection, unless otherwise specified. MSC were also isolated from the BM of the *CMV-R26R* or *BMP-2-Lac Z* mice and transplanted into wild-type female littermates. The *BMP-2-Lac Z and CMV-R26R* mice were generated as described in the supporting information data or previously reported [32].

BLI analyses

BLI imaging was performed using an IVIS 200 imaging system (Caliper Life Sciences). All images were collected 15 minutes after D-Luciferin (150 mg/kg) intraperitoneal injection. Additional information on the BLI analyses is available in the supporting information data. BLI signaling at the fracture tibia site region of interest (ROI), measured as integrated photons/second/cm^2/steradian (sr), was normalized by subtracting the background signal found in an equal ROI in the contralateral intact tibia. Imaging data were analyzed using the LivingImages2.20.1 (Xenogen Corp., Hopkinton, MA, http://www.caliperls.com).

Luciferase-expressing adenoviruses and MSC infection

An adenoviral vector that encodes the *Firefly luciferase* under the control of a cytomegalovirus promoter was used to generate highly purified (CsCl gradient) viruses as previously described [33]. All the experiments were performed using a multiplicity of infection of 1,000 in MSC cultured for 7 days. Additional information is provided in the supporting information data.

Biomechanical testing

Fractured tibias were dissected 14 days after fracture, wrapped in phosphate-buffered saline-embedded gauze, and stored at -80°C until analysis. The bone ends were embedded with polymethylmetacrylate and loaded into the electroforce-based system ELF 3100 (Bose Corp., Framingham, MA, http://www.bose.com). The displacement rate was at 0.25 mm/minute, and a force-displacement curve was recorded to calculate the ultimate distraction (maximum distraction at failure), ultimate force (maximum force at failure), toughness (area under the curve), and stiffness (maximum slope) using the WinTestControl Software (Bose).

Histology and in situ hybridization

Tibias were dissected 7 and 14 days after fracture and histologically prepared, and the entire callus was sectioned (6 μm). The callus center was identified as the largest diameter by H&E staining and analyses were performed within 20 sections from the center. In situ hybridization analysis was performed as previously

reported [34]. Plasmid with insertion of mouse Collagen (II)-alpha1-chain (*Col2a1*) was provided by D. Kingsley (Stanford University); mouse Collagen (I)-α-1-chain (*Col1a1*) and mouse *Osteocalcin* were provided by G. Karsenty (Columbia University). Probe for mouse Collagen (X)alpha1chain (*Col10a1*) was generated as previously described [35]. Images were taken using an Olympus BX51 microscope with a DP71 camera (Tokyo, http://www.olympus-global.com), imported into Adobe Photoshop (Adobe Systems, San Jose, CA, http://www.adobe.com), and formatted without using any imaging enhancement.

Micro-computed tomography analysis of fracture calluses

Tibia fractures were dissected 14 days after fracture, and following removal of the pin, were scanned using micro-computed tomography (μCT) (Scanco Medical μCT40; Akron, OH, http://www.scanco.com). μCT imaging was obtained at 55-kilovolt peak, 145-μA, 300-millisecond integration time using 6-μm voxel resolution along 5.2-mm length centered at the fracture line with a total scanning time of approximately 1 hour [36]. To determine material type from μCT scans, a parametric thresholding study was performed by serial μCT scanning and histological analysis as reported in the supporting information data.

Circulating and callus cytokine measurements

Sera were obtained from mice that received MSC transplant and controls at days 1, 3, and 7 after fracture. Tumor necrosis factor-α (TNF-α), interleukin-1 β (IL-1β), interleukin-10 (IL-10), interleukin-13 (IL-13), and interleukin-6 (IL-6) levels were determined using LINCOplex immunoassay (Linco Research, St. Charles, MO, http://www.lincoresearch.com). Total RNA obtained using Trizol and PureLinK columns (Invitrogen, Carlsbad, CA, http://www.invitrogen.com) from dissected calluses 3 and 7 days after fracture was reversed transcribed using SuperScript III reverse transcriptase (Invitrogen) and Oligod(T)16 (Applied BioSystems, Foster City, CA, http://www.appliedbiosystems.com). *TNF-α* mRNA expression was measured by quantitative reverse-transcription polymerase chain reaction (RT-PCR) (MyIQ-Single-Color-RT-PCR-System; Bio-Rad, Hercules, CA, http://www.bio-rad.com) using Syber Green as previously described [37]. PCR primers for *TNF-α* amplification were as follows: 5′-CCACCA CGCTCTTCTGTCTAC-3′ and 5′-GGCTACAGGCTTGTCACT CG-3′. Samples were run in triplicates, and data were normalized to β-actin expression and analyzed using the $2^{-\Delta\Delta CT}$ method and expressed as fold of increases compared with the average of control that did not undergo transplantation, which was given the value of 1.

X-Gal staining

X-Gal staining was performed as previously described with some modifications [32]. Briefly, the fractured tibia was dissected, briefly fixed with 0.4% paraformaldehyde (PFA), and stained at room temperature with X-Gal staining solution. To achieve specific localization of cells that express prokaryotic (*Escherichia coli*) β-galactosidase, pH of the reacting solution was adjusted to selectively favor its activity over that of the mammalian enzyme [38, 39]. After staining, samples were fixed with 4% PFA for 24 hours and paraffin embedded, and sections were counterstained using nuclear Fast Red as previously described [32, 35]. CMV-R26R-Lac Z-MSC (1×10^5) were placed in 10 μl medium in a 24-well plate and after 1 hour, 500 μl of medium was added; cells were cultured for 24 hours and X-Gal stained as previously reported [35].

Statistics

Data are expressed as mean ± SD. Statistical analyses were performed using Student's *t* test, and one-way or two-way analysis of variance followed by post hoc multiple comparison testing. The relationship between number of transplanted MSC and BLI signal was analyzed using a dose-response sigmoid curve. GraphPad Prism 5 Software was used (GraphPad Software, San Diego, http://www.graphpad.com). Statistical significance was set at $p < .05$.

Supporting Information Data

Supporting information data are available.

RESULTS

Systemically Transplanted MSCs: In Vivo Dynamic and Time-Dependent Recruitment at the Fracture Site

To assess the in vivo MSC dynamic trafficking and homing in response to a pathological tibia fracture cue, 1×10^6 MSC-β-Act-Luc, constitutively expressing *luciferase*, were transplanted into a mouse with stabilized tibia fracture and sequential BLI imaging was performed from day 1 to day 14 after fracture/transplantation. As depicted in Figure 1A (left panel), 1 day after the fracture/transplantation MSC-β-Act-Luc were visualized in the lungs. On day 3 after the fracture, we observed that MSC began to localize at the fractured leg site (right tibia) where they persisted up to 14 days after the fracture/transplantation (Fig. 1A, left panel). Semiquantitative analysis of the BLI signal of luciferase-tagged MSC over the fractured leg, was time-dependent, increasing progressively from day 1 to day 7, without any further increase at day 14.

The Presence of CXCR4 Is Essential for MSC Homing at the Fracture Site

The finding that MSCs have the ability to migrate to an injured tibia implies that they own specific homing signal(s). Although CXCR4 has been involved in the hematopoietic stem cell engraftment and cancer cell metastasis, its role in MSC homing still needs to be defined [18, 19, 40–42]. In our study, using primary cultures of unpassaged MSC immunodepleted of hematopoietic cells, we first found that ∼30% of MSC express CXCR4 (34.2% ± 4.7%, $n = 4$ MSC cultures obtained from the BM of at least 4 mice for each culture). Second, we separated, using CXCR4 immunoselection, the MSC population as MSC-CXCR4(+) and MSC-CXCR4(−) populations that were injected into a mouse with a tibia fracture. One day after fracture both MSC-CXCR4(+) and MSC-CXCR4(−) had a localization pattern similar to the unselected MSC (Fig. 1A). However, at day 3, MSC-CXCR4(−) were not capable of homing to the fracture site, whereas the MSC-CXCR4(+) showed an intense signal (Fig. 1A, middle and right panels). A similar scenario was observed at day 7 and day 14 following the fracture/transplantation (Fig. 1, middle and right panels). As shown in Figure 1B, semiquantitative analysis of the BLI signal confirmed that the MSC-CXCR4(−) migration to the fracture site at any studied time point was negligible; whereas MSC-CXCR4(+) showed a time-dependent increase of MSC-luciferase signal at the fractured tibia. Our data demonstrate that systemically transplanted MSC are capable of homing at the fracture site and the migration is dependent on the presence of CXCR4.

Dose-Dependent MSC Homing at the Fracture Site

To assess the dose-dependent MSC homing at the fracture site, we systemically infused MSC transduced with an adenoviral vector expressing *luciferase* (MSC-Adn-Luc) into mice with a tibia fracture. We reasoned that since adenoviruses do not integrate in the host genome, and expression is lost in dividing cells, the luciferase signal would exclusively assess

A

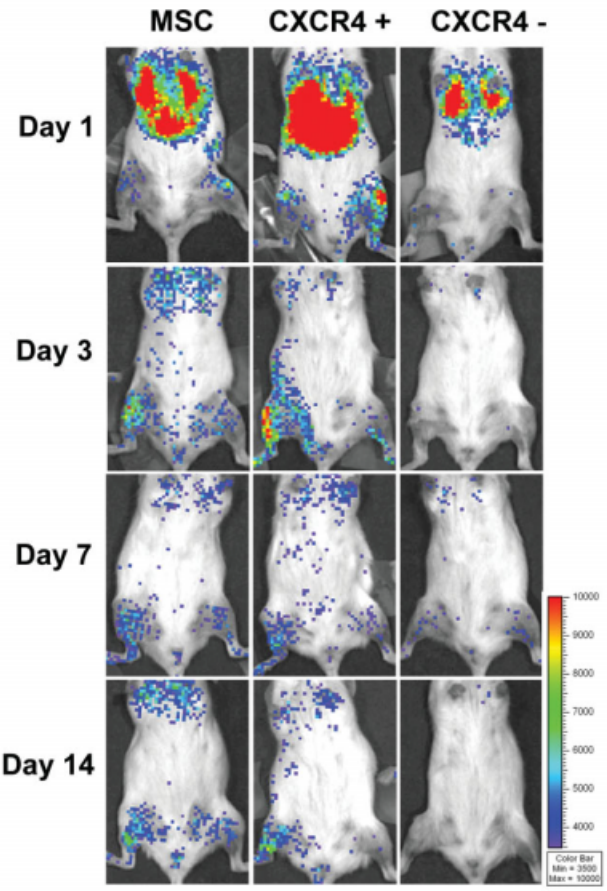

B

	MSC	CXCR4+	CXCR4-	P Value (ANOVA)
Day 3 post-fracture	5317 ± 3468[a] n=14	6464 ± 4814[b] n=8	546 ± 433 n=8	0.0037
Day 7 post-fracture	7093 ± 2041[a] n=6	8526 ± 4202[b] n=4	133 ± 745 n=3	0.0057
Day 14 post-fracture	6508 ± 5350 n=5	18149 ± 6100[a,c] n=3	2440 ± 806 n=3	0.0109

Figure 1. MSCs migrate to the fracture site in a time- and CXCR4-dependent manner. **(A):** Bioluminescence (BLI) was performed at days 1, 3, 7, and 14 after fracture/transplantation in mice with tibia fracture that received a transplant of either 10^6 MSC-β-Act-Luc (MSC) (left panel), MSC-β-Act-Luc-CXCR4$^+$ (CXCR4(+)) (middle panel), or MSC-β-Act-Luc-CXCR4$^-$ (CXCR4(−)) (right panel). Graded color bar indicates BLI signal intensity expressed as photons/seconds/cm^2/steradian (sr). **(B):** BLI signal semiquantitative analysis. Signal at the fracture tibia site region of interest (ROI), measured as photons/seconds/cm^2/sr, was normalized by subtracting the background signal found in an equal ROI in the contralateral unfractured tibia. [a], $p < .05$ versus CXCR4 group; [b], $p < .01$ versus CXCR4 group; [c], $p < .05$ versus MSCs by Tukey post-test. Abbreviations: ANOVA, analysis of variance; MSC, mesenchymal stem cells.

the MSC migration to the fracture site. As shown in supporting information Figure 3A, in mice with fractured tibia that received transplants of increasing doses of MSC-Adn-Luc (from 5×10^3 to $1{,}000 \times 10^3$ MSC) and BLI imaged 3 days later, we found that MSC homing was dose-dependent. Interestingly, we found the ED_{50} to be a dose of 300×10^3, with a plateau at 700×10^3 without any significant increase at a dose of $1{,}000 \times 10^3$ (supporting information Fig. 3C). This

Table 1. MSCs improve the biomechanical properties of the fracture callus

	No cells ($n = 5$)	MSCs ($n = 6$)
Toughness (N-mm)	0.138 ± 0.044	0.425 ± 0.143[b]
Ultimate force (N)	1.803 ± 0.488	2.492 ± 0.829
Stiffness (N/mm)	17.790 ± 8.861	12.000 ± 7.591
Ultimate displacement (mm)	0.124 ± 0.045	0.308 ± 0.148[a]

Fourteen days after tibial fracture, calluses from mice that received a MSC transplant or controls (no cells) were dissected and subjected to distraction-to-failure biomechanical testing.
[a]$p < .05$ versus no cells; [b]$p < .01$ versus no cells by Student's t test.
Abbreviations: MSCs, mesenchymal stem cells; N, Newton.

finding indicates that MSC migration to the injured site reaches a saturation point and a limiting mechanism that needs further investigation can be hypothesized.

MSC Improve the Biomechanical Properties of the Fracture Callus

A critical feature of bone healing is that the regenerated tissue provides sufficient strength to the injured limb to regain function. To investigate whether MSC improved the callus material properties we performed distraction-to-failure biomechanical testing. Dissected calluses from MSC recipient mice (MSC), as well as control calluses from mice that did not receive MSC (no cells), were subjected to a gradual distraction force until they broke. As shown in Table 1, calluses of mice that received MSC had increased toughness and ultimate displacement compared with controls. The peak force was not different in the two groups, although there was a trend toward a decrease of callus stiffness in the mice that received MSC. Taken together, these data indicate that MSC improved the callus material properties, making the tissue less brittle by decreasing the structural rigidity.

MSC Effects on Callus Size and Morphology

To determine material type (bone and soft tissue) from μCT scans, a parametric threshold study of an entire callus was performed by serial μCT scanning and histological analyses (in situ hybridizations for *Collagen 1, Collagen 10,* and trichrome blue and safranin O/Fast Green staining) (supporting information data). Mice that received MSC transplant displayed a significant increase of the total volume, as well as total bone, soft tissue, new bone, and callus volumes and callus mineralization content compared with controls (Fig. 2A). The three-dimensional reconstructions of the entire calluses as well as the sagittal sections showed remarkable differences in the size and morphology of the new mineralized callus in mice that received MSC versus controls. As shown in Figure 2B, the most notable differences were that (a) a large callus surrounded the fractured bone edges as well as the intact cortical bone in the calluses from mice that received a transplant of MSC, but remained limited to the ends of the bone segments in the controls (compare panels B1 with B5 and B3 with B7); and (b) there was a continuous net of the creeping callus bridging the fracture gap in MSC recipient mice versus the limited connectivity observed in the controls (compare panels B2 with B6 and B4 with B8). These findings indicate that MSC transplant, by providing a more organized bridge between the bone ends, improves the repairing process and therefore its material properties.

MSC Effects on Callus Histology

We next analyzed the callus histology as well as bone and cartilaginous marker expressions at days 7 and 14 after the fracture and MSC transplant. H&E staining analyses showed that at 7 days, the calluses from mice that received MSC transplant were bigger than controls and demonstrated larger areas of cartilage-like tissue (Fig. 3A). In situ hybridization for *Collagen 2* and *Collagen 10* expression as well as safranin O staining revealed a more abundant presence of either chondrocytes or hypertrophic chondrocytes in the calluses from mice that received MSC transplant, indicating that the fracture repair in those mice more predominately proceeded through an endochondral ossification process than controls (Fig. 3A). When evaluated at 14 days after the fracture, *Collagen 10* expression was also consistently higher in mice that received MSC than controls and, at this time, it was associated with an increase of *Collagen 1* expression indicating that the endochondral callus progressed to bone formation (Fig. 3B).

MSC Distribution Within the Callus

To analyze the cellular distribution of transplanted MSC within the callus, fractured mice received a MSC transplant from *CMV-R26R* mice, and 7 days after fracture-transplantation dissected calluses were Lac-Z stained. As shown in supporting information Figure 4, CMVR26R-Lac Z-MSC express stainable β-galactosidase activity, indicating this as a suitable reporter system for MSC. As negative control for the Lac Z staining protocol, 7-day postfracture calluses from wild-type mice were Lac-Z stained. As shown in the supporting information Figure 5, no staining was detectable, indicating that the protocol used did not result in any background.

As shown in Figure 4A, we found that transplanted CMVR26R-Lac Z-MSC localized within specific areas of the callus, in particular within the fracture ridge, the endosteum close to the fracture rim, and the BM. Counterstaining the calluses with safranin O/Fast Green (Fig. 5B), we identified that MSC localized within the endosteal callus in the areas of most active bone formation. Higher magnification of these areas showed that the Lac-z–positive MSC (stained in blue) were embedded in the bone matrix (stained in green) as osteoblasts within the newly forming bone (Fig. 5C) or as newly formed osteocytes with abundant cytoplasm (Fig. 5D). As shown in supporting information Figure 6, in situ hybridization analysis confirmed that within the margins of the woven bone, some of the Lac Z-positive MSC expressed also *osteocalcin,* confirming their ability to differentiate into osteoblasts. Our findings indicate that transplanted MSC localize within different and specific niches of the callus, and the number of MSC within the newly forming bone seems to be limited compared with the significant effects of MSC on the callus biomechanical properties. This observation led us to hypothesize that the contributions of MSC to fracture healing are likely through multiple mechanisms that include, but are not limited to, callus mineralization.

MSC Contribute to the Callus Initiation by Expressing BMP-2

To determine the contribution of MSC to the initial phase of the callus formation, we analyzed whether transplanted MSC were capable of expressing bone morphogenic protein 2 (BMP-2) within the callus. BMP-2 is highly expressed during fracture healing and is essential for the callus initiation [43]. In fact, in mice null for BMP-2 expression in limb mesenchyme progenitors, the earliest steps of fracture healing are blocked and mice lack fracture healing [43]. For this purpose,

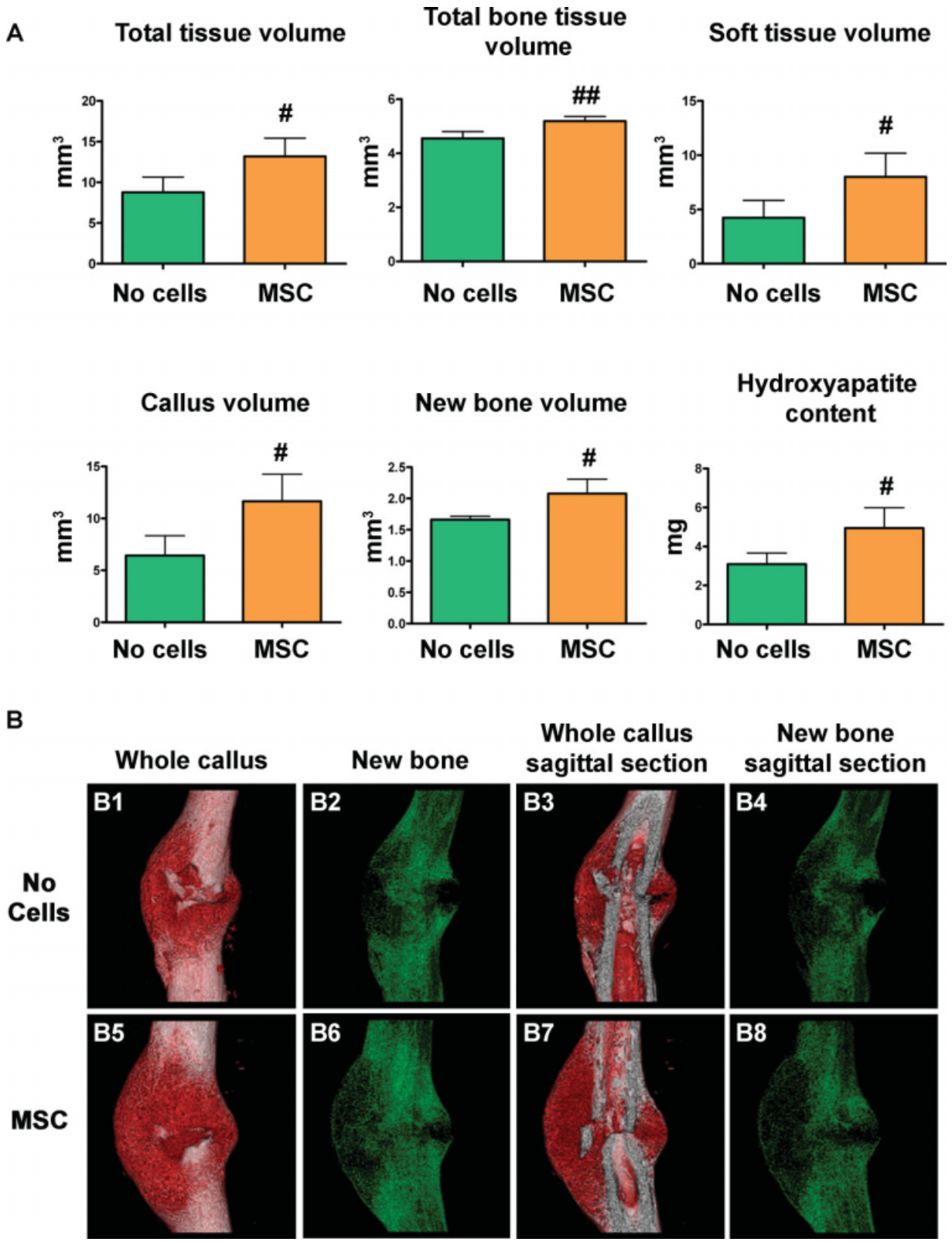

Figure 2. MSC transplantation increases callus size and changes callus morphology. **(A):** Micro-computed tomography (μCT) analyses were performed 14 days after fracture in calluses dissected from mice that received MSC transplant and controls (no cells). Callus volume and new bone volume were calculated after subtracting the cortical bone volume, respectively, from the total volume and the total bone tissue volume. #, $p < .05$ versus no cells; ##, $p < .01$ versus no cells by Student's t test. No cells, $n = 3$; MSC, $n = 6$. **(B):** Three-dimensional reconstruction of whole calluses (B1, B2, B5, B6) and sagittal sections (B3, B4, B7, B8) was obtained 14 days after tibial fracture in calluses from mice that received a MSC transplant or control mice that did not undergo transplantation (no cells). Material type analysis of new bone and soft tissue was determined by a histological-based thresholding of the μCT imaging scans. Abbreviation: MSC, mesenchymal stem cells.

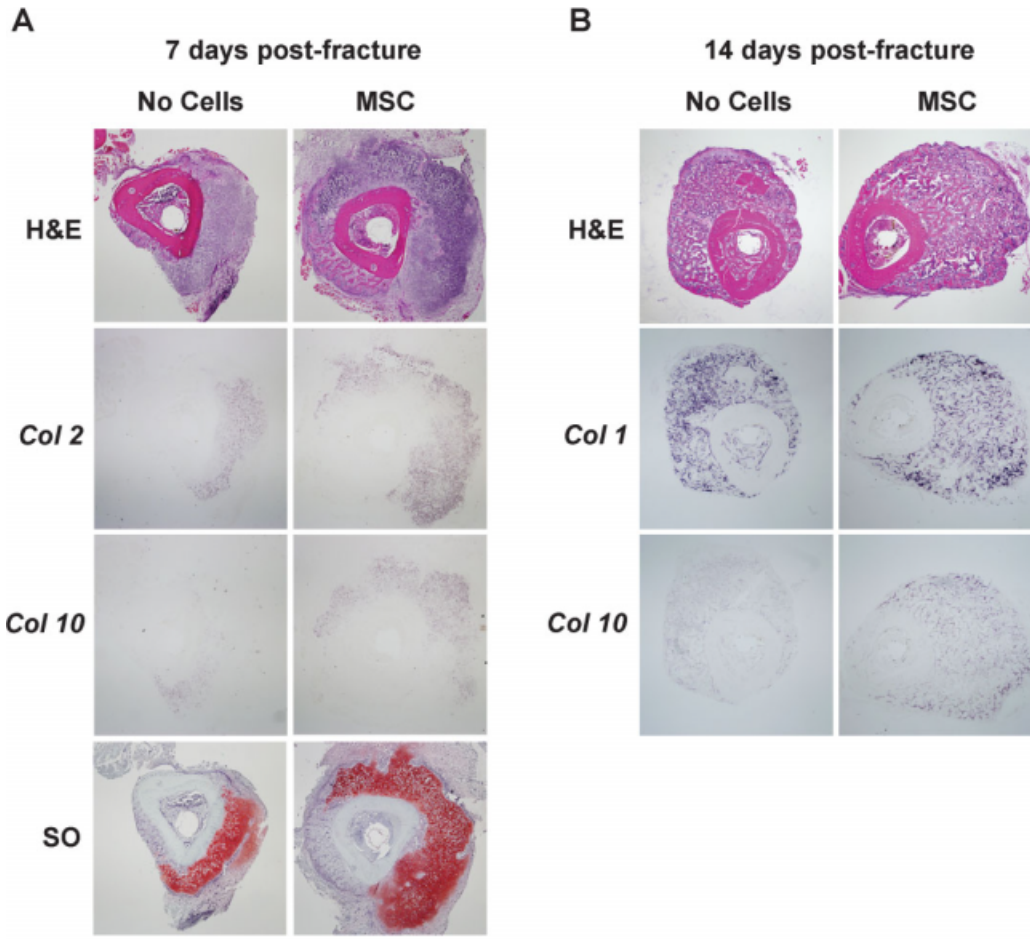

Figure 3. MSC transplantation increases the cartilaginous and bone content of the callus. **(A):** Transversal sections of 7-day postfracture calluses were subjected to H&E and safranin O staining and in situ hybridization for *Collagen-2* and *Collagen-10*. **(B):** Fourteen days after fracture transversal sections were subjected to H&E staining and in situ hybridization for *Collagen-1* and *Collagen-10*. The entire callus was sectioned (6-μm-thick sections), the center of the callus was identified by the largest diameter of callus size by H&E staining, and further analyses were performed within 20 sections from the center. Analyses were done in at least 5 sections for each probe or staining. Sections were obtained from at least 3 mice for each group. Abbreviations: Col 1, collagen 1; Col 2, collagen 2; Col 10, collagen 10; H&E, hematoxylin & eosin; MSC, mesenchymal stem cells; SO, safranin O. Magnifications presented are $\times$40.

we obtained MSC from *BMP-2-Lac-Z* mice genetically modified using a bacterial artificial chromosome (BAC) system to be β-gal reporters for BMP-2 expression [32]. BMP-2-Lac Z-MSC were transplanted into fractured mice, and calluses were dissected 7 days after the fracture and Lac-Z stained. We found that BMP-2-Lac-Z-MSC localized within the fracture rim and more peculiarly along the endosteum adjacent to the fracture edges (Fig. 5A-B). This pattern was similar to the pattern observed in the fractured mice that received a transplant of CMVR26R-Lac Z-MSC, although the mice that received a transplant of BMP-2-Lac Z-MSC lacked the Lac Z staining within the BM cells. Our data indicate that transplanted MSC localize at the fracture site and are capable of expressing BMP-2, an essential gene for initiating the fracture repair process. To determine the endogenous BMP-2 expression at the same fracture healing stage, calluses were obtained 7 days after fracture from *BMP-2-Lac Z* fractured mice and Lac Z stained. As shown in Figure 5C–5D, we found that BMP-2 is highly expressed at the fracture rim and interestingly no expression was detectable at the endosteal site. This observation may indicate that the endosteum is a peculiar niche where the transplanted MSC engraft and express BMP-2.

MSC Transplant Modulates the Systemic and Local Inflammatory Responses

To determine whether the beneficial contributions of MSC to the fracture healing were associated with an anti-inflammatory action, we sequentially determined the circulating levels of a set of cytokines in the serum of mice that received a MSC transplant or controls. As shown in Figure 6, over the first week after the fracture, MSC transplant selectively downregulated the serum levels of TNF-α and IL-1β, abolishing the injury-induced inflammatory response found in the control fractured mice. The MSC anti-inflammatory action was targeted to specific cytokines; in fact, MSC had no effect on IL-13 and IL-10 at any time but had a significant effect at reducing IL-6 levels only at day 3 after fracture (Fig. 6C–6E). MSC had similar effects on the local mRNA expression of TNF-α that was decreased in the calluses from mice that received MSC transplant compared with controls at day 3 (MSC: 1.278 $\pm$ 1.741-fold of change; control: 3.78 $\pm$ 3.006-fold of change; $p < .05$; $n = 6$) and day 7 (MSC: 0.670 $\pm$ 0.315-fold of change; control: 2.729 $\pm$ 2.334-fold of change; $p < .05$; $n = 6$) after fracture.

Discussion

In our studies, we have characterized, in living animals, the dynamic migration of MSC in response to a bone fracture and determined that this specific migration at the site of injury is driven by CXCR4. We have also demonstrated that MSC transplantation induces a biomechanical improvement of the healing process that is associated with an increase in the callus volumes and cartilaginous and bone contents. We have found that MSC engraft into specific niches of the callus expressing the fracture repair initiator BMP-2 and that the delivery of MSC has a specific systemic and local anti-inflammatory effect. In summary, our report provides a comprehensive assessment of the contributions of transplanted MSC to the fracture healing process.

There is a significant body of evidence that links MSC to tissue regeneration, including bone and cartilage [20]. However, in vivo studies have been performed primarily using post-mortem analyses; as a result longitudinal evaluations of MSC dynamic in living animals are scarce [15]. Furthermore, studies have been limited in the attempt to demonstrate one of the regenerative effects of MSC, mostly the differentiation into bone, lacking an ample evaluation of the multiple actions of MSC. The regeneration of damaged tissue implies that different responses converge at the damaged area. The regenerative cells need to be recruited at the injury site, control the injury-induced responses, and eventually contribute to the repair. In our studies, we have demonstrated that MSC exert their regenerative properties by contributing to each of the stages of fracture healing. Transplanting MSC tagged with luciferase in combination with BLI analysis, we have demonstrated that MSC migrate to a fracture site and migration is time- and dose-dependent. Recruitment of circulating progenitor cells to the site of injury occurs as a normal biological process during the fracture process [44]. We hypothesize that MSC injected systemically migrate to the fracture site using a similar injury-related recruitment mechanism. Gao et al. using ^{111}I-indium-MSC investigated the MSC dynamic for only 48 hours after cell infusion into normal noninjured rats [15]. The authors found that after injection, cells distributed into the lungs and the liver and a vasodilator increased the liver localization [15]. We found similar results in our short-term BLI studies, but our long-term analyses in fractured mice allowed us to determine that 3 days after the fracture/transplantation, MSC were specifically recruited at the fracture site where they remained up to 14 days. Thus, the use of MSC transplantation seems to be a valid strategy to allow a noninvasive increase of viable progenitors at a fracture site.

We have found that fracture MSC migration is dependent on the presence of CXCR4. There are discordant data on whether MSC express CXCR4 and its role in MSC migration [18, 19, 40–42]. Differences in culture passages may be the reason for such discordances; in fact, cell passaging causes a downregulation of CXCR4 expression and loss of MSC homing [18, 45, 46]. We have used primary cultures of

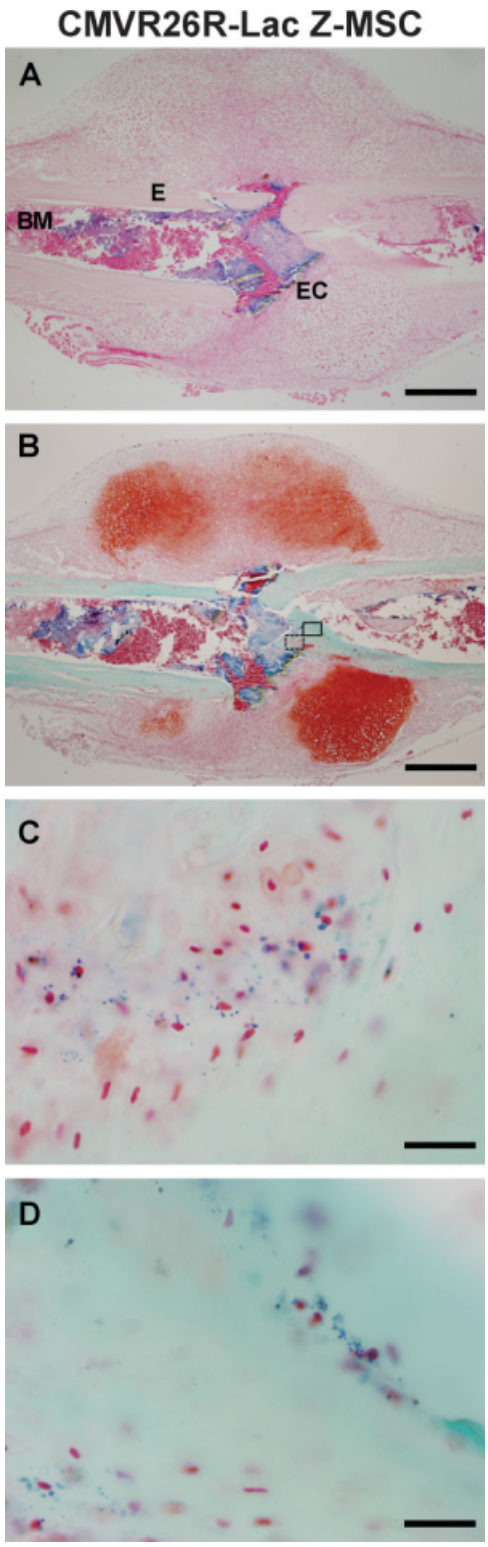

Figure 4. Transplanted MSCs localize within specific niches of the fracture callus. CMVR26R-Lac Z-MSC (10^6) were transplanted into fractured mice, and calluses dissected 7 days after fracture and X-gal stained. **(A):** Paraffin sections of the β-galactosidase (β-gal)-stained calluses were counterstained with nuclear Fast Red showing MSC localization into specific areas of the fracture callus. **(B):** Paraffin sections of β-gal-stained calluses were counterstained with safranin O/Fast Green. **(C):** Higher magnification of the dashed line box depicted in **(B)** showed MSC embedded into the bone matrix as osteoblasts. **(D):** Higher magnification of the solid line box depicted in **(B)** showed MSC also integrated into the bone matrix as newly formed osteocytes. **(A, B):** Scale bar = 500 μm; **(C, D)** scale bar = 33 μm. Sections were obtained from at least 3 mice. Abbreviations: BM, bone marrow; E, endosteum; EC, endosteal callus; MSC, mesenchymal stem cells.

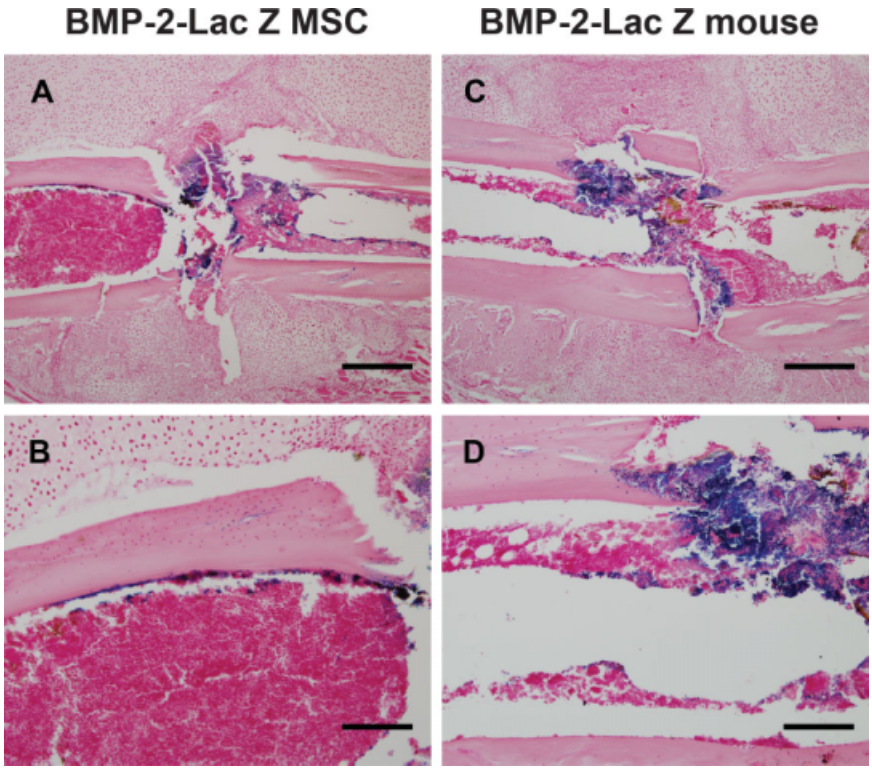

Figure 5. Transplanted MSC express BMP-2 within the fracture and localize at the endosteal site of the callus. **(A):** BMP-2-Lac Z-MSC (10^6) were transplanted into fractured mice and 7 days after fracture the calluses were dissected and X-gal stained. Paraffin sections were counterstained with nuclear Fast Red showing that MSC localize and express BMP-2 into the fracture rim and endosteum. **(B):** Higher magnification of **(A)**, showing the endosteal localization of MSCs expressing BMP-2. **(C):** BMP-2-Lac Z mice were fractured; 7 days after fracture calluses were dissected and β-gal stained, and paraffin sections were counterstained with nuclear Fast Red and showed BMP-2 expression at the fracture ridge. **(D):** Higher magnification of the fracture rim showing expression of BMP-2. **(A, C):** Scale bar = 500 μm; **(B, D)** scale bar = 200 μm. Sections were obtained from at least 3 mice. Abbreviations: BMP-2, bone morphogenic protein-2; MSC, mesenchymal stem cells.

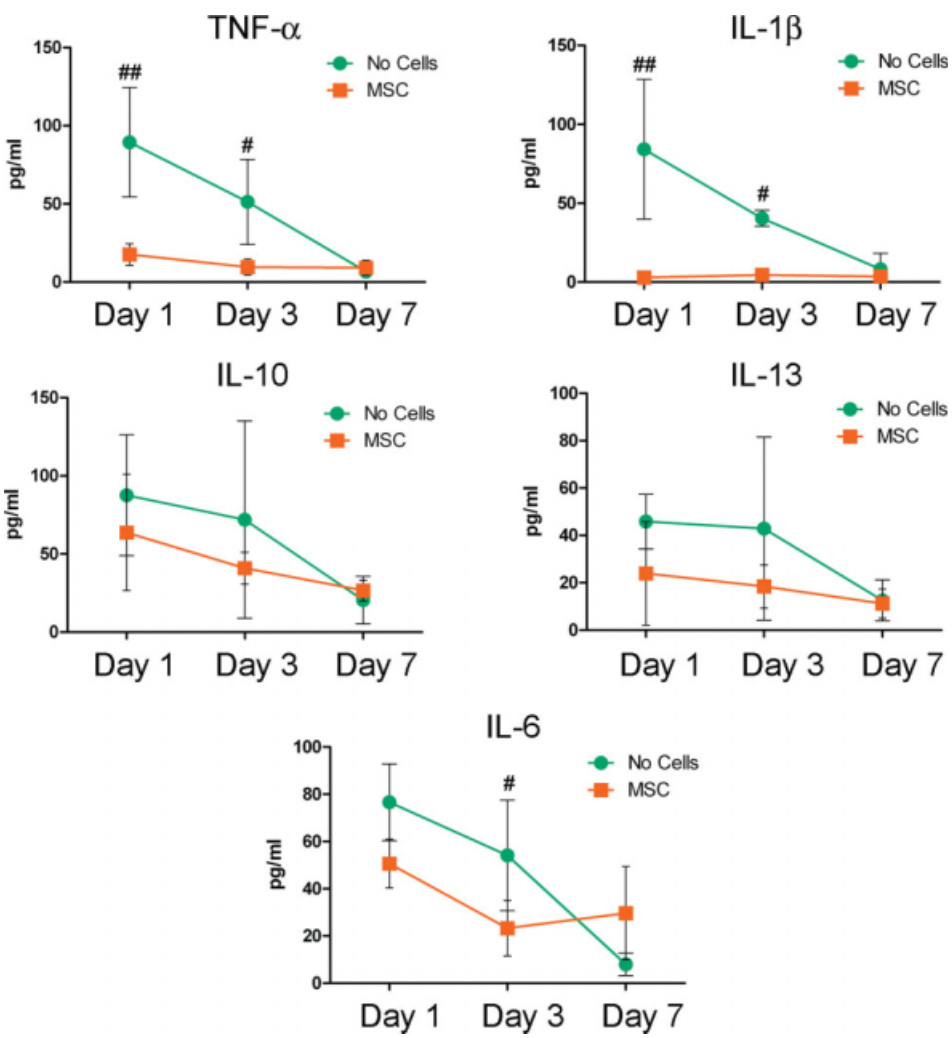

Figure 6. Transplanted MSC have specific systemic anti-inflammatory effects on the cytokines released after tibia fracture. Cytokines were measured in sera obtained 1, 3, and 7 days after fracture from mice that received a MSC transplant or controls (no cells) by LINCOplex immunoassay. Sera were obtained from at least 4 mice for each group at each corresponding time. #, $p < .05$ versus control at the corresponding time; ##, $p < .01$ versus control at the corresponding time by Tukey post-test. Abbreviations: IL-1β, interleukin-1 β; IL-6, interleukin-6; IL-10, interleukin-10; IL-13, interleukin-13; MSC, mesenchymal stem cells; TNF-α, tumor necrosis factor-α.

unpassaged MSC immunodepleted of hematopoietic cells and found a consistent CXCR4 expression in ~30% of the MSC population. Cheng et al. have recently reported that MSC recruitment was enhanced in a rat model of myocardial infarction by retrovirally overexpressing CXCR4 in MSC that lacked CXCR4 [47]. In our study, we have found that, without any CXCR4 manipulation, native primary cultured MSCs are capable of homing at a fracture site in a CXCR4-dependent manner.

In our study, we found that MSC transplantation improves the fracture healing by increasing the material toughness of the callus and causing it to be less brittle. The observed biomechanical material data were consistent with the μCT imaging that showed in MSC recipient mice some remarkable differences in the callus geometry that was larger with more organized bridging structures characterized by soft tissue and new bone. Histological analyses confirmed that the fracture healing in MSC recipient mice progressed through more cartilage and newly mineralized bone than controls. Tibia fractures necessitate a long period for healing. Optimization of clinical management can reduce the healing time, however it has been pointed out that even if osteogenic cells at the fracture site are working at full capacity, they will not heal the defect if too few cells are present, nor will any drug, directed at enhancing bone formation, be effective since maximal osteogenesis per cell is already occurring [48]. Our studies provide evidence that even in a normal fracture-healing tibia model, MSC transplantation enhances the repair process, supporting the use of MSC to provide a critical number of regenerative cells to achieve the desired bone-repairing results in patients with high-energy fractures. Although some nonunion animal models are available, these models are based either on mice with genetic defects that lead to repair impairments, or by creating large bone gaps or stripping the periosteum to decrease the number of regenerative progenitors. None of these models reflects the mechanisms for nonunions found in patients. Furthermore, the healing times in those models are largely inconsistent, making problematic the interpretation of results when multiple experimental groups are studied. On the other hand, the stabilized fracture tibia model we have used has a consistent healing time, and having found that, in this model, MSCs have several positive effects we are optimistic about the prospect of using MSC in nonunions.

In our studies using Lac Z-tagged MSC, we found that transplanted MSC localize along the margins of woven bone where they assume the morphology of active osteoblasts, express osteocalcin, and associate with the endosteal surface. Interestingly, MSC did not localize within the periosteal callus, although the overall size of the callus of mice that received MSC transplant was larger and showed larger areas of newly forming bone. This observation led us to pursue studies aimed at determining whether the MSC regenerative effects were not related exclusively to their differentiative abilities into bone but also to their contributions to the initiation of the healing process. Our study is the first to report that systemically injected MSC localize at the fracture site where they are capable of expressing BMP-2, an essential initiator of the fracture repair process [43]. One interesting finding from our study is that MSC expressing BMP-2 localize very distinctly at the endosteum site. The endosteum maintains the bone homeostasis and participates in the fracture healing process, and a lack of the endosteal callus formation is critical in the pathogenesis of nonunions [49–51]. Several cells form the endosteal niche, including osteoblasts, CXCL12-abundant reticular (CAR) cells, MSC, and hematopoietic stem cells. There is a large body of evidence that supports the notion that the endosteal osteoblasts provide a variety of factors that regulate the hematopoietic stem cell number and function (reviewed in [52, 53]). It has been hypothesized that in the endosteal niche CAR cells together with osteoblasts, and potentially other cell types, generate a hypoxic environment that maintains the hematopoietic stem cells in a quiescent state [53]. The inhibitory effect of MSC on cell proliferation in vitro raises the possibility of a role for MSC in maintaining the hematopoietic stem cells in this quiescent state [54]. On the other hand, hematopoietic stem cells regulate MSC induction into osteoblasts in vitro as well as ex vivo [55]. Our knowledge of the MSC niches within native tissues is very poor and even less is known about the MSC niches after transplantation. Our study provides evidence for the homing of circulating transplanted MSC in response to a fracture injury cue into the endosteal niche, where they express BMP-2. It is plausible that MSC expressing CXCR4 are recruited to the endosteal niche by CAR cells. We hypothesize that MSC within the endosteal niche can either differentiate into osteoblasts, or, through a paracrine action, control the injury-related inflammatory response. It will be of great interest to evaluate in future longitudinal studies the contributions of MSC through the entire reparative process.

Several studies have shown that MSC have the ability to suppress the inflammatory response in vitro as well as in vivo (reviewed in [20, 22]). These anti-inflammatory effects were induced through paracrine mechanisms that shifted the tissue milieu from a proinflammatory to an anti-inflammatory state [23–26]. During the tissue repairing process a precise temporal and spatial resolution of the inflammatory response is critical to limit the tissue injury, to prevent the development of fibrosis, and ultimately to promote regeneration. Uncontrolled inflammation plays a critical role in the pathogenesis of nonunions. Traditional anti-inflammatory drugs that block the cytokine response in toto are unable to direct and selectively control the process and may actually have negative effects on the healing process. In our study, we have found that the beneficial effects of MSC transplantation on fracture regeneration are associated with a selective effect on systemic and local cytokine production. MSC, as selective modulators of the inflammatory response, may become the target of new therapies to enhance the healing process in patients with nonunions.

Summary

In summary, we have determined that transplanted MSC improve the fracture repair process and we have elucidated several of the mechanisms involved in these beneficial effects. We have characterized the dynamic of MSC migration and the essential role of CXCR4, we have found the niches for MSC recruitment at the injury site, and we have determined that MSC contribute to the fracture healing by expressing BMP-2 and modulating the injury-related inflammatory response. Our findings provide some critical information to implement the development of MSC-based therapies in patients with poorly healing fractures.

Acknowledgments

This work was supported by a National Institutes of Health Grant 5R01DK070929-02 (to A.S.). We acknowledge the support of the Vanderbilt Emphasis Program and the Endocrine Society Summer Research Fellowships (to B.L.). We recognize the technical support of the Biomedical Research Imaging Center at University of North Carolina at Chapel Hill, the Vanderbilt Institute

of Imaging Science, and the Vanderbilt's Institutional Immunohistochemistry Core at Vanderbilt University. We thank K. Shimer for her early participation in the BLI analyses. We acknowledge Ron Chandler for his technical advice. We thank D. Kingsley and G. Karsenty for providing reagents.

Disclosure of Potential Conflicts of Interest

The authors indicate no potential conflicts of interest.

References

1 Keating JF, Blachut PA, O'Brien PJ et al. Reamed nailing of Gustilo grade-IIIB tibial fractures. J Bone Joint Surg 2000;82:1113–1116.
2 Einhorn TA. Enhancement of fracture-healing. J Bone Joint Surg Am 1995;77:940–956.
3 Marsh D. Concepts of fracture union, delayed union, and nonunion. Clin Orthop 1998:S22–S30.
4 Praemer A, Furner S, Rice DP. Musculoskeletal Conditions in the United States. 2nd ed. Rosemont HL, ed. Park Ridge, IL: The American Academy of Orthopaedic Surgeons; 1999, p 83–87.
5 Morshed S, Corrales L, Genant H et al. Outcome assessment in clinical trials of fracture-healing. J Bone Joint Surg Am 2008;90(suppl 1): 62–67.
6 Einhorn TA. The cell and molecular biology of fracture healing. Clin Orthop Relat Res 1998:S7–S21.
7 Pittenger MF, Mackay AM, Beck SC et al. Multilineage potential of adult human mesenchymal stem cells. Science 1999;284:143–147.
8 Marcacci M, Kon E, Moukhachev V et al. Stem cells associated with macroporous bioceramics for long bone repair: 6- to 7-year outcome of a pilot clinical study. Tissue Eng 2007;13:947–955.
9 Quarto R, Mastrogiacomo M, Cancedda R et al. Repair of large bone defects with the use of autologous bone marrow stromal cells. N Engl J Med 2001;344:385–386.
10 Hernigou P, Mathieu G, Poignard A et al. Percutaneous autologous bone-marrow grafting for nonunions. Surgical technique. J Bone Joint Surg Am 2006;88(suppl 1; pt 2):322–327.
11 Hernigou P, Poignard A, Beaujean F et al. Percutaneous autologous bone-marrow grafting for nonunions. Influence Of The Number And Concentration of Progenitor Cells. J Bone Joint Surg Am 2005;87: 1430–1437.
12 Hernigou P, Poignard A, Manicom O et al. The use of percutaneous autologous bone marrow transplantation in nonunion and avascular necrosis of bone. J Bone Joint Surg Br 2005;87:896–902.
13 Tseng SS, Lee MA, Reddi AH. Nonunions and the potential of stem cells in fracture-healing. J Bone Joint Surg Am 2008;90(suppl 1): 92–98.
14 Chapel A, Bertho JM, Bensidhoum M et al. Mesenchymal stem cells home to injured tissues when co-infused with hematopoietic cells to treat a radiation-induced multi-organ failure syndrome. J Gene Med 2003;5:1028–1038.
15 Gao J, Dennis JE, Muzic RF et al. The dynamic in vivo distribution of bone marrow-derived mesenchymal stem cells after infusion. Cells Tissues Organs 2001;169:12–20.
16 Barbash IM, Chouraqui P, Baron J et al. Systemic delivery of bone marrow-derived mesenchymal stem cells to the infarcted myocardium: feasibility, cell migration, and body distribution. Circulation 2003;108: 863–868.
17 Zou YR, Kottmann AH, Kuroda M et al. Function of the chemokine receptor CXCR4 in haematopoiesis and in cerebellar development. Nature 1998;393:595–599.
18 Wynn RF, Hart CA, Corradi-Perini C et al. A small proportion of mesenchymal stem cells strongly expresses functionally active CXCR4 receptor capable of promoting migration to bone marrow. Blood 2004;104:2643–2645.
19 Von Lüttichau I, Notohamiprodjo M, Wechselberger A et al. Human adult CD34- progenitor cells functionally express the chemokine receptors CCR1, CCR4, CCR7, CXCR5, and CCR10 but not CXCR4. Stem Cells Dev 2005;14:329–336.
20 Granero-Molto F, Weis JA, Longobardi L et al. Role of mesenchymal stem cells in regenerative medicine: application to bone and cartilage repair. Expert Opin Biol Ther 2008;8:255–268.
21 Le Blanc K, Gotherstrom C, Ringden O et al. Fetal mesenchymal stem-cell engraftment in bone after in utero transplantation in a patient with severe osteogenesis imperfecta. Transplantation 2005;79: 1607–1614.
22 da Silva Meirelles L, Caplan AI, Nardi NB. In search of the in vivo identity of mesenchymal stem cells. Stem Cells 2008;26:2287–2299.
23 Ortiz LA, Gambelli F, McBride C et al. Mesenchymal stem cell engraftment in lung is enhanced in response to bleomycin exposure and ameliorates its fibrotic effects. Proc Natl Acad Sci U S A 2003; 100:8407–8411.
24 Zappia E, Casazza S, Pedemonte E et al. Mesenchymal stem cells ameliorate experimental autoimmune encephalomyelitis inducing T-cell anergy. Blood 2005;106:1755–1761.
25 Parekkadan B, van Poll D, Suganuma K et al. Mesenchymal stem cell-derived molecules reverse fulminant hepatic failure. Plos One 2007;2:e941.
26 Bartholomew A, Sturgeon C, Siatskas M et al. Mesenchymal stem cells suppress lymphocyte proliferation in vitro and prolong skin graft survival in vivo. Exp Hematol 2002;30:42–48.
27 Le Blanc K, Frassoni F, Ball L et al. Mesenchymal stem cells for treatment of steroid-resistant, severe, acute graft-versus-host disease: a phase II study. Lancet 2008;371:1579–1586.
28 Bruder SP, Jaiswal N, Ricalton NS et al. Mesenchymal stem cells in osteobiology and applied bone regeneration. Clin Orthop 1998: S247–S256.
29 Petite H, Viateau V, Bensaid W et al. Tissue-engineered bone regeneration. Nat Biotechnol 2000;18:959–963.
30 Bonnarens F, Einhorn TA. Production of a standard closed fracture in laboratory animal bone. J Orthop Res 1984;2:97–101.
31 Spagnoli A, Longobardi L, O'Rear L. Cartilage disorders: potential therapeutic use of mesenchymal stem cells. Endocr Dev 2005;9: 17–30.
32 Chandler RL, Chandler KJ, McFarland KA et al. Bmp2 transcription in osteoblast progenitors is regulated by a distant 3′ enhancer located 156.3 kilobases from the promoter. Mol Cell Biol 2007;27:2934–2951.
33 Fowler M, Virostko J, Chen Z et al. Assessment of pancreatic islet mass after islet transplantation using in vivo bioluminescence imaging. Transplantation 2005;79:768–776.
34 Deal KK, Cantrell VA, Chandler RL et al. Distant regulatory elements in a Sox10-beta GEO BAC transgene are required for expression of Sox10 in the enteric nervous system and other neural crest-derived tissues. Dev Dyn 2006;235:1413–1432.
35 Spagnoli A, O'Rear L, Chandler RL et al. TGF-beta signaling is essential for joint morphogenesis. J Cell Biol 2007;177:1105–1117.
36 Reynolds DG, Hock C, Shaikh S et al. Micro-computed tomography prediction of biomechanical strength in murine structural bone grafts. J Biomech 2007;40:3178–3186.
37 Longobardi L, O'Rear L, Aakula S et al. Effect of IGF-I in the chondrogenesis of bone marrow mesenchymal stem cells in the presence or absence of TGF-beta signaling. J Bone Miner Res 2006;21: 626–636.
38 Nolan GP, Fiering S, Nicolas JF et al. Fluorescence-activated cell analysis and sorting of viable mammalian cells based on beta-D-galactosidase activity after transduction of Escherichia coli lacZ. Proc Natl Acad Sci U S A 1988;85:2603–2607.
39 Devine MJ, Mierisch CM, Jang E et al. Transplanted bone marrow cells localize to fracture callus in a mouse model. J Orthop Res 2002; 20:1232–1239.
40 Honczarenko M, Le Y, Swierkowski M et al. Human bone marrow stromal cells express a distinct set of biologically functional chemokine receptors. Stem Cells 2006;24:1030–1041.
41 Chamberlain G, Wright K, Rot A et al. Murine mesenchymal stem cells exhibit a restricted repertoire of functional chemokine receptors: comparison with human. Plos One 2008;3:e2934.
42 Fox JM, Chamberlain G, Ashton BA et al. Recent advances into the understanding of mesenchymal stem cell trafficking. Br J Haematol 2007;137:491–502.
43 Tsuji K, Bandyopadhyay A, Harfe BD et al. BMP2 activity, although dispensable for bone formation, is required for the initiation of fracture healing. Nat Genet 2006;38:1424–1429.
44 Kumagai K, Vasanji A, Drazba JA et al. Circulating cells with osteogenic potential are physiologically mobilized into the fracture healing site in the parabiotic mice model. J Orthop Res 2008;26: 165–175.
45 Peled A, Petit I, Kollet O et al. Dependence of human stem cell engraftment and repopulation of NOD/SCID mice on CXCR4. Science 1999;283:845–848.
46 Rombouts WJ, Ploemacher RE. Primary murine MSC show highly efficient homing to the bone marrow but lose homing ability following culture. Leukemia 2003;17:160–170.
47 Cheng Z, Ou L, Zhou X et al. Targeted migration of mesenchymal stem cells modified with CXCR4 gene to infarcted myocardium improves cardiac performance. Mol Ther 2008;16:571–579.

48 Bruder SP, Fink DJ, Caplan AI. Mesenchymal stem cells in bone development, bone repair, and skeletal regeneration therapy. J Cell Biochem 1994;56:283–294.
49 Szulc P, Delmas PD. Bone loss in elderly men: increased endosteal bone loss and stable periosteal apposition. The Prospective Minos Study. Osteoporos Int 2007;18:495–503.
50 Markel MD, Wikenheiser MA, Chao EY. A study of fracture callus material properties: relationship to the torsional strength of bone. J Orthop Res 1990;8:843–850.
51 Rutten S, Nolte PA, Korstjens CM et al. Low-intensity pulsed ultrasound increases bone volume, osteoid thickness and mineral apposition rate in the area of fracture healing in patients with a delayed union of the osteotomized fibula. Bone 2008;43:348–354.
52 Mitsiadis TA, Barrandon O, Rochat A et al. Stem cell niches in mammals. Exp Cell Res 2007;313:3377–3385.
53 Wilson A, Trumpp A. Bone-marrow haematopoietic-stem-cell niches. Nat Rev 2006;6:93–106.
54 Glennie S, Soeiro I, Dyson PJ et al. Bone marrow mesenchymal stem cells induce division arrest anergy of activated T cells. Blood 2005; 105:2821–2827.
55 Jung Y, Song J, Shiozawa Y et al. Hematopoietic stem cells regulate mesenchymal stromal cell induction into osteoblasts thereby participating in the formation of the stem cell niche. Stem Cells 2008;26:2042–2051.


See www.StemCells.com for supporting information available online.